Centralized Inverted Decoupling for TITO Processes

Juan Garrido
Universidad de Córdoba
Dpto. de Informática
14071 Córdoba (Spain)
juan.garrido@uco.es

Francisco Vázquez
Universidad de Córdoba
Dpto. de Informática
14071 Córdoba (Spain)
fvazquez@uco.es

Fernando Morilla
UNED
Dpto. de Informática y Automática
28040 Madrid (Spain)
fmorilla@dia.uned.es

Abstract

This paper presents a new approach of centralized control for TITO processes which is based on the structure of inverted decoupling. After defining the general expressions of this methodology, it is indicated how to specify the desired open loop transfer function in order to achieve free offset error and the desired performance (gain margins or phase margins). Then, the case of processes with all their elements as first order plus time delay (FOPTD) systems is studied in more detail because it generates two PI controllers and two derivative compensators with time delay, which can be implemented easily. If the process elements are more complex it is proposed to approximate them to FOPTD systems. The methodology is applied to two simulation examples and a real experimental lab process. Comparisons with other authors show its effectiveness.

1. Introduction

Most industrial processes are multivariable systems, that are much more difficult to control compared with SISO counterparts because of the existence of interactions between the measurement signals and the control signals. Two-input two-output (TITO) system is one of the most prevalent categories of multivariable systems, because there are real processes of this nature or because a complex process has been decomposed in 2×2 blocks [1, 2, 3, 4] with non negligible interactions between its inputs and outputs. According to the interactions and the control requirements, a diagonal controller (decentralized control) or a full matrix controller (centralized control) can be adopted.

In general, centralized control is advisable when these interactions are significant. There are two different approaches of centralized control. The first of them uses a decoupling network D(s) to reduce the undesirable cross-couplings, plus a decentralized controller $K_d(s)$ [5, 6, 7, 8]. The resulting centralized controller is $K(s)=D(s)\cdot K_d(s)$. The second one uses a pure centralized strategy. Under the paradigm of "decoupling control" some of these methodologies propose to find a K(s) such that the closed loop transfer matrix $G(s)\cdot K(s)\cdot[I+G(s)\cdot K(s)]^{-1}$ is decoupled over some desired bandwidth. This goal is ensured if the open loop transfer matrix $G(s)\cdot K(s)$ is diagonal. For this reason, the techniques used in decoupling control are very similar to the techniques used to design decouplers.

Lieslehto, in [9], presented an n×n centralized control and its particularization to PID controllers based on Internal Model Control (IMC) SISO design. A more experimental work [10, 11] approaches the multivariable PID controller tuning as an optimization problem, where it is necessary to define the desired closed loop transfer function matrix. In [12, 13] a decoupler with integral action is designed and then it is approximated by a PID network including delay. In [14] a new approach of decoupling is presented on the basis of equivalent transfer function matrix.

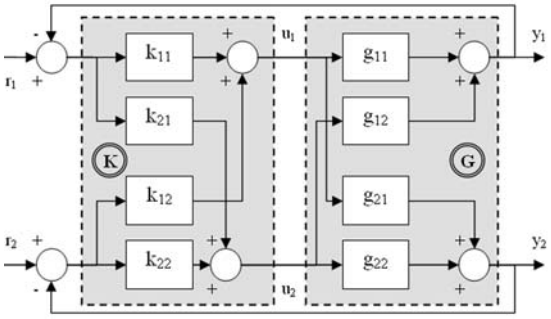

Figure 1: 2×2 conventional centralized control with four controllers.

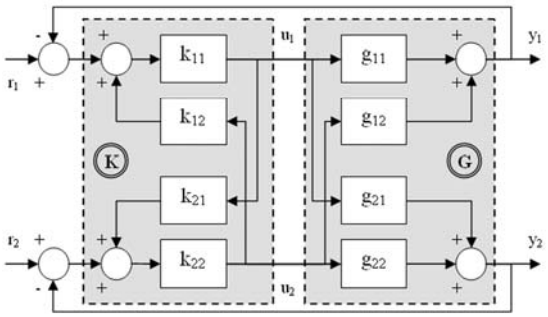

Figure 2: 2×2 inverted centralized control with four controllers.

All these methodologies use the conventional scheme of centralized control depicted in Fig. 1, which has

978-1-4244-6849-2/10/$26.00 ©2010 IEEE

received considerable attention in both control theory and applications for several years. However, this paper proposes another centralized control scheme called "centralized inverted decoupling", which is showed in Fig. 2. It is based on the structure of inverted decoupling, which is rarely mentioned in the literature. In [7] inverted decoupling is shown to be a form of ideal decoupling. A comparative study of simplified, ideal and inverted decoupling is carried out in [15], and in [16] it is improved for processes with multiple time delays and nonminimum-phase zeros.

Using the scheme of Fig. 2 it is possible to achieve the desired requirements with very simple $k_{ij}(s)$ elements in the controller. Additionally, the elements of the open loop process $G(s)\cdot K(s)$ are much less complicated than using the conventional centralized decoupling control.

This paper presents this new approach to decoupling problem for 2×2 stable plants with time delays based in inverted decoupling. The methodology is discussed in Section 2. The proposed method is applied to two simulation processes and a real laboratory plant in Section 3. Finally, conclusions are summarized in Section 4.

2. Centralized inverted decoupling control

Considering the unity output feedback 2×2 control system in Fig. 2, and assuming that the open loop transfer matrix $L(s)=G(s)\cdot K(s)$ should be diagonal, the elements $k_{ij}(s)$ of the inverted centralized control are given by

$$k_{11}=\frac{l_1}{g_{11}} \qquad k_{12}=\frac{-g_{12}}{l_1} \qquad k_{21}=\frac{-g_{21}}{l_2} \qquad k_{22}=\frac{l_2}{g_{22}} \qquad (1)$$

where the operator s has been omitted. The proof is explained in the appendix A. $l_1(s)$ and $l_2(s)$ are the desired open-loop transfer functions. The main advantage of (1) is the simplicity of the k_{ij} elements in comparison with the corresponding expressions (2) for the conventional centralized control of Fig.1.

$$K=\begin{pmatrix} k_{11} & k_{12} \\ k_{21} & k_{22} \end{pmatrix}=\frac{\begin{pmatrix} g_{22}l_1 & -g_{12}l_2 \\ -g_{21}l_1 & g_{11}l_2 \end{pmatrix}}{g_{11}g_{22}-g_{12}g_{21}} \qquad (2)$$

The controller elements of (1) do not contain sum of transfer functions, whereas the controller elements of (2) may result very complicated even if the elements of the system have simple dynamics. In addition, the open loop transfer functions $l_i(s)$ may keep very simple in such a way that the performance requirements can be specify easily.

Nevertheless, the structure of centralized inverted decoupling control presents an important disadvantage: because of stability problems it cannot be applied to processes with multivariable right half plane (RHP) zeros, that is, RHP zeros in the determinant of the process transfer matrix G(s). For internal stability these RHP zeros should appear in open-loop transfer functions of L(s). In the conventional centralized decoupling control, RHP zeros of the determinant of G(s) can be included into the open loop transfer functions $l_i(s)$. But it is not possible using centralized inverted decoupling control, because such RHP zeros would appear as unstable poles in some controller elements $k_{ij}(s)$ according to (1). Only if the multivariable RHP zero is associated to an only output, and therefore it is included into the process transfer functions of a same row, inverted decoupling control can be applied because the RHP zero will be cancelled.

In order to obtain the four k_{ij}, it is only necessary to specify the two transfer functions $l_i(s)$. They can be chosen freely as long as the controller elements are realizable. Next subsections treat different design considerations to solve the presented problem.

2.1. Controller realizability

The realizability requirement for the controller is that its elements should be proper, causal and stable. For processes with time delays or RHP zeros, the direct calculation of the controller can lead to elements with prediction or RHP poles. This problem is well discussed in [16] for inverted decoupling of TITO processes. Apart from the scheme of Fig. 2, there is an alternative configuration for centralized inverted control. This is showed in Fig. 3 and the equations of the controller elements in this case are given by

$$k_{11}=\frac{-g_{11}}{l_1} \qquad k_{12}=\frac{l_2}{g_{21}} \qquad k_{21}=\frac{l_1}{g_{12}} \qquad k_{22}=\frac{-g_{22}}{l_2} \qquad (3)$$

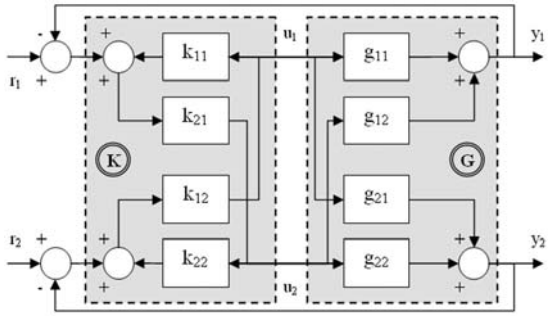

Figure 3: alternative 2×2 inverted centralized control with four controllers.

Next, the conditions that a specified configuration (Fig. 2 or Fig. 3) needs to satisfy in order to be realizable are commented. Also the constraints on the open-loop transfer function $l_i(s)$ are indicated. There are three aspects to take into account and to be inspected by row:

1 - Non causal time delays τ_{ij} must be avoided in controller elements. If g_{ik} is the transfer function of the row *i* with the smallest time delay τ_{ik}, the element k_{ki} of K(s) should be selected to be in the direct path between the process and the reference error. In addition, the time delay (τ_i) of the l_i transfer function must be in the range between the minimum and maximum time delays of the same row.

$$\min(\tau_{ij}) \le \tau_i \le \max(\tau_{ij}) \quad j=1,2 \qquad (4)$$

where $\tau(f(s))$ represents the time delay of a generic function f(s) and *min* represents the minimum function, and *max*, the maximum function.

2 - Decoupler elements must be proper, that is, the relative degrees r_{ij} must be greater or equal than zero. Similarly to the previous case, the element k_{ki} should be in the direct path if the transfer function g_{ik} has the smallest relative degree r_{ik} of the row *i*. In addition, the relative degree (r_i) of the l_i transfer function must fulfil

$$\min(r_{ij}) \le r_i \le \max(r_{ij}) \quad j = 1,2 \qquad (5)$$

3 - When some transfer function g_{im} has a RHP zero, the element k_{mi} of K(s) should not be selected in the direct path, in order to avoid this zero becomes a RHP pole in some controller element. When the zero appears in all elements of the same row, it is necessary to check its multiplicity η_{ij} in each element. Again, if g_{ik} is the transfer function of the row *i* with the smallest RHP zero multiplicity η_{ik}, the element k_{ki} should be selected to be in the direct path. This RHP zero must appear in the l_i open-loop transfer function with a multiplicity (η_i) that fulfils

$$\min(\eta_{ij}) \le \eta_i \le \max(\eta_{ij}) \quad j = 1,2 \qquad (6)$$

From (4), (5) and (6), note that when the value (time delay, relative degree or RHP zero multiplicity) is shared by both transfer functions of the row, there are more possibilities to choose the configuration, but the flexibility (time delay or relative degree) of the open-loop process l_i is limited to the common value of row.

When two elements of K(s) have to be selected necessarily in the same column to satisfy the previous conditions in both rows, there is no realizable configuration. Then, it is necessary to insert an additional block N(s) between the system G(s) and the inverted controller K(s) in order to modify the process and to force the non-realizable elements into realizability. Then, centralized inverted control would be applied to the new process $G_N(s)=G(s)\cdot N(s)$.

N(s) is a diagonal block with the necessary extra dynamics. If there are no realizability problems in the row *i*, the N(i,i) element is equal to the unity. If the non-realizability comes from an element with a non causal time delay, an additional time delay ($e^{-\tau s}$) is inserted in the corresponding diagonal element of N(s). If it comes from a RHP zero z, which has become unstable pole, the following element is used in N(s)

$$\left(\frac{-s+z}{s+z^*}\right)^{\eta_i} \qquad (7)$$

where z* is the complex conjugate of z. And if it comes from a properness problem, a simple stable pole with the adequate multiplicity can be inserted as follows

$$\frac{1}{(\lambda s+1)^{r_i}} \qquad (8)$$

Generally it is preferable to add the minimum extra dynamics. Therefore, after checking the necessary additional dynamics of each configuration (Fig. 2 or Fig. 3), it is chosen that one with less RHP zeros or time delays in N(s).

2.2. How to specify the $l_i(s)$?

Every open-loop transfer function $l_i(s)$ used in equation (1) or (3) must take into account the dynamic of two processes $g_{i1}(s)$ and $g_{i2}(s)$ to get realizability, and the achievable performance specifications of the corresponding SISO closed-loop system. Since the closed loop must be stable and without steady-state errors due to setpoint or load changes, the open-loop transfer function $l_i(s)$ must contain an integrator. Then, the following general expression for $l_i(s)$ is proposed:

$$l_i(s) = k_i \, \bar{l}_i(s) \, \frac{1}{s} \, e^{-s\tau_i} \qquad \text{with } \tau_i \ge 0 \qquad (9)$$

The time delay should fulfil condition (4). Parameter k_i becomes a tuning parameter in order to met design specifications and the $\bar{l}_i(s)$ must be a rational transfer function taking account of the not cancellable dynamic of g_{i1} and g_{i2} and the conditions (5) and (6).

Next, the attention is directed to the three most common cases included in table 1.

Table 1. The three most common open-loop transfer functions according to the process to be controlled.

Process	$\bar{l}_i(s)$	$l_i(s)$
Stable and minimum phase	1	$\frac{k_i}{s} e^{-s\tau_i}$
Stable and non-minimum phase zero in the same row	$\frac{-(s-z)}{s+z}$	$\frac{-k_i(s-z)}{s(s+z)} e^{-s\tau_i}$
Stable and minimum phase plus integrator	$\frac{s+z_i}{s}$	$\frac{k_i(s+z_i)}{s^2} e^{-s\tau_i}$

2.3. How to determine the parameters of $l_i(s)$?

This question is analyzed for each of the cases of table 1. The parameters of $l_i(s)$ are determined depending on desired specifications of the closed-loop system. A similar study is carried out in [12].

Case 1: The processes of the same row are stable and minimum phase systems. $\bar{l}_i(s)$ and $l_i(s)$ are given by the first row in table 1. It is enough to impose relative stability specification (gain or phase margins) to the function $l_i(s)$ in order to guarantee the stability of the closed-loop transfer function $h_i(s)=l_i(s)/(1+l_i(s))$. It can be shown that $l_i(s)$ gets the following stability margins at following frequencies:

$$\phi_m = 90 - \frac{180\, k_i\, \tau_i}{\pi} \quad ; \quad \omega_{cp} = k_i \qquad (10)$$

$$A_m = \frac{\pi}{2\, k_i\, \tau_i} \quad ; \quad \omega_{cg} = \frac{\pi}{2\, \tau_i} \qquad (11)$$

Then both stability margins are related by:

$$\phi_m = 90 - \frac{90}{A_m} \qquad (12)$$

If phase margin ϕ_m (less than 90º) is specified or gain margin A_m (greater than 1), the value of k_i is directly determined as follows:

$$k_i = \frac{\pi(90 - \phi_m)}{180\ \tau_i} \quad (13)$$

$$k_i = \frac{\pi}{2\ A_m\ \tau_i} \quad (14)$$

Increasing k_i makes the loop faster but with smaller values of phase margin and gain margin. If no delay is present, $\tau_i = 0$, the function $l_i(s)=k_i/s$ shows a phase margin of 90º and an infinite gain margin, independent of k_i value. In this case, the closed-loop transfer function has the typical shape of a first order system:

$$h_i(s) = \frac{k_i/s}{1 + k_i/s} = \frac{1}{T_i\ s + 1} \quad (15)$$

with time constant $T_i = 1/k_i$. Then, in order to determine k_i it is enough to specify the time constant of the closed-loop system.

Case 2: The common non-minimum phase zero of the row cannot be cancelled, it must appear in $\bar{l}_i(s)$, then $\bar{l}_i(s)$ and $l_i(s)$ are given by the second row in table 1. In these conditions, it can be shown that

$$A_m = \frac{\omega_{cg}}{k_i} \quad (16)$$

at frequency ω_{cg}, that verifies the following equation

$$\tan(\omega_{cg}\tau_i) = \frac{1 - \frac{\omega_{cg}^2}{z^2}}{2\frac{\omega_{cg}}{z}} \quad (17)$$

If no delays are present, $\tau_i = 0$, the A_m specification can be replaced by time response specifications, because closed loop transfer function is

$$h_i(s) = \frac{-k_i\ (s - z)}{s^2 + (z - k_i)\ s + k_i\ z} \quad (18)$$

Its poles are characterized by the undamped natural frequency and the damping factor

$$\omega_n = \sqrt{k_i\ z} \quad ; \quad \delta = \frac{z - k_i}{2\sqrt{k_i\ z}} \quad (19)$$

and then, it is possible to fix the value δ with $k_i<z$.

Case 3: The processes are stable, except in s=0, and minimum phase systems. The pole in s=0 must appear in $\bar{l}_i(s)$, then $\bar{l}_i(s)$ and $l_i(s)$ are given by the third row in table 1. In these conditions,

$$A_m = \frac{\omega_{cg}^2}{k_i\ \sqrt{\omega_{cg}^2 + z_i^2}} \quad (20)$$

at frequency ω_{cg}, that verifies the following equation

$$\text{arc tg}\ \frac{\omega_{cg}}{z_i} - \omega_{cg}\ \tau_i = 0 \quad (21)$$

If there is not delay, $\tau_i = 0$,

$$h_i(s) = \frac{k_i\ (s + z_i)}{s^2 + k_i\ s + k_i\ z_i} \quad (22)$$

Its poles are characterized by the undamped natural frequency and the damping factor

$$\omega_n = \sqrt{k_i\ z_i} \quad ; \quad \delta = \sqrt{\frac{k_i}{4\ z_i}} \quad (23)$$

Subsequently, if the value of z_i is fixed, with k_i it is possible to modify the values of ω_n and δ. Particularly, it is sufficient to select $k_i=4z_i$ in order to achieve poles with critical damping (δ=1) and $\omega_n=2z_i$.

2.4. About the controllers $k_{ij}(s)$

Substituting equations (9) into (1) yields

$$k_{ii}(s) = k_i \frac{\bar{l}_i(s)}{g_{0ii}(s)} \cdot \frac{1}{s}\ e^{-s(\tau_i - \tau_{ii})} \quad (24)$$

$$k_{ij}(s) = -\frac{1}{k_i} \frac{g_{0ij}(s)}{\bar{l}_i(s)} \cdot s\ e^{-s(\tau_{ij} - \tau_i)} \quad (25)$$

where $g_{0ij}(s)$ is the delay free part of $g_{ij}(s)$. A very similar result is obtained substituting (9) into (3).

Two resulting controller elements (24) have integral action and therefore they could be approximated by PID controllers. The other two controllers (25) are compensators with derivative action plus time delay. Note that the derivative action should be filtered to avoid the amplification of high frequency noise and to be implementable. Depending of the desired $l_i(s)$ and the $g_{ij}(s)$ of the process, the $k_{ij}(s)$ elements can be very difficult to implement. In this case the use of model reduction techniques can be suggested. In next subsection, these techniques are used in order to get PID structure and filtered derivative action plus time delay.

2.5. Using PID structure

If it is intended that controllers become ideal PID plus delay, it is necessary to force the following structure in the controller elements (24)

$$k_{ii}^{PID}(s) = \frac{k_i}{s}\ \left(K_{Dii}\ s^2 + K_{Pii}\ s + K_{Iii}\right) e^{-s\tau(k_{ii})} \quad (26)$$

where it appears the controller delay $\tau(k_{ii})$ and its proportional (K_{Pii}), integral (K_{Iii}) and derivative (K_{Dii}) gains. Instead of reducing the controller given by (24), authors propose to remove the delay, the integrator and the gain k_i and to apply the model reduction to the inverse simplified expression m_{ii} as follows:

$$k_{ii}(s) = k_i\ \left(m_{ii}(s)\right)^{-1}\ \frac{1}{s}\ e^{-s\tau(k_{ii})} \quad (27)$$

$$m_{ii}(s) = \frac{\tilde{b}_{ii}(s)}{\tilde{a}_{ii}(s)}\ \left(\bar{l}_i(s)\right)^{-1} \cong \frac{b_o}{a_2\ s^2 + a_1\ s + a_o} \quad (28)$$

In this way, the controller gains will be $K_{Pji} = a_1/b_o$, $K_{Iji} = a_o/b_o$ y $K_{Dji} = a_2/b_o$. Similarly, to reduce the controller elements (25) to a structure of filtered derivative action plus time delay (29), it is suggested to apply the model reduction to (31). In this way, $K_{Dji} = b_o/a_o$ and $N_{ij} = a_1/a_o$.

$$k_{ij}^{D}(s) = -\frac{s}{k_i}\ \left(\frac{K_{Dij}}{N_{ij}s+1}\right) e^{-s\tau(k_{ij})} \quad (29)$$

$$k_{ij}(s) = -\frac{s}{k_i}\ \left(m_{ij}(s)\right) e^{-s\tau(k_{ij})} \quad (30)$$

$$m_{ij}(s) = \frac{\tilde{b}_{ij}(s)}{\tilde{a}_{ij}(s)} \left(\bar{l}_i(s)\right)^{-1} \cong \frac{b_o}{a_1 s + a_o} \quad (31)$$

2.6. FOPTD systems

Since almost all industry processes are open loop stable and exhibit non oscillatory behaviour for unit step inputs, higher order transfer functions can be simplified to first order plus time delay (FOPDT) model before the control design. In this way it is assumed that all process transfer functions can be described by

$$g_{ij}(s) = \frac{k_{ij}}{T_{ij}s+1} e^{-\tau_{ij}s} \quad (32)$$

The transfer functions are stable and minimum phase systems, so it is possible to specify $\bar{l}_i(s)$ according to the case 1. Consequently, using the inverted scheme of Fig.2, the $k_{ii}(s)$ elements are PI controllers (33), and the other two are filtered derivative compensators plus time delay (34). It is necessary to select the time delay of $l_i(s)$ equal to the time delay of $g_{ii}(s)$.

$$k_{ii}(s) = \frac{k_i}{k_{ii}} \frac{(T_{ii}s+1)}{s} = \frac{K_{Pii}s + K_{Iii}}{s}$$
$$K_{Pii} = T_{ii}\frac{k_i}{k_{ii}} \quad ; \quad K_{Iii} = \frac{k_i}{k_{ii}} \quad (33)$$

$$k_{ij}(s) = -\frac{k_{ij}}{k_i} \frac{s}{(T_{ij}s+1)} e^{-(\tau_{ij}-\tau_i)s} = \frac{-K_{Dij}s}{N_{ij}s+1} e^{-\tau(k_{ij})s}$$
$$K_{Dij} = \frac{k_{ij}}{k_i} \quad ; \quad N_{ij} = T_{ij} \quad ; \quad \tau(k_{ij}) = \tau_{ij} - \tau_i \quad (34)$$

When it is possible to approximate the transfer functions of the process by FOPTD systems, authors propose to do it and to use the simple equations (33) and (34) to calculate the $k_{ij}(s)$ elements. Nevertheless, if the $g_{ij}(s)$ have pure integrators, common RHP zeros or other elements which make difficult the previous reduction, authors advise to approximate the final $k_{ij}(s)$ elements (two for PID controllers and the other two for lead-lag compensator with filtered derivative action plus time delay) according to the previous section.

3. Examples

In this section the proposed methodology is applied to two simulation processes very cited in literature. Also, its effectiveness is verified in a real quadruple tank plant.

3.1. Wood and Berry column

The Wood-Berry binary distillation column plant [17] is a multivariable system that has been studied extensively. The process has important delays in its elements. It is described by the transfer matrix:

$$G_{WB}(s) = \begin{pmatrix} \frac{12.8}{16.7s+1}e^{-s} & \frac{-18.9}{21.0s+1}e^{-3s} \\ \frac{6.6}{10.9s+1}e^{-7s} & \frac{-19.4}{14.4s+1}e^{-3s} \end{pmatrix} \quad (35)$$

The two open-loop transfer functions $l_1(s)$ y $l_2(s)$ are chosen following the first row of table 1, and the time delays τ_1=1 and τ_2=3 are selected. Gain margins of A_{m1}=6 and A_{m2}=4 are specified and according to (14) k_1=0.262 and k_2=0.131 are obtained. Then, since the four $g_{ij}(s)$ are FOPTD systems, the expressions (33) and (34) can be used to design the controllers (Table 2).

Table 2. Controller parameters for the Wood and Berry column.

k(s)	K_P	K_I	K_D	N	τ
k_{11}	0.342	0.0205	0	0	0
k_{22}	-0.097	-0.0067	0	0	0
k_{12}	x	x	-72.193	21	2
k_{21}	x	x	50.42	10.9	4

Next figures show the step response of the closed-loop system of the proposed controller in comparison with other control methods in the literature. Specifically, the methodology is compared with the Smith predictor of Wang [11], the decoupler network plus decentralized PI control of Tavakoli [6] and the conventional centralized PID control by decoupling of the current authors in [12].

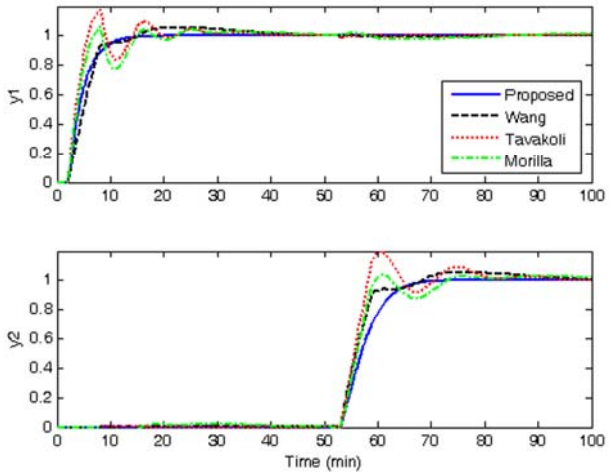

Figure 4: Outputs of the step response of Wood-Berry column.

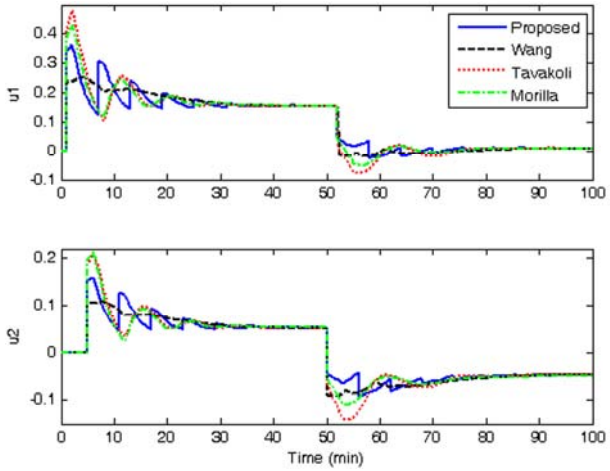

Figure 5: Control signals of the step response of Wood-Berry column.

Fig. 4 shows that the proposed methodology does not show an oscillatory behaviour in the outputs and there is no interaction in any loop. Although the response seems a bit slower in the second loop, the settling time is better. Fig. 5 shows the control signals responses. The Smith predictor of Wang presents the best ones, while the others show an oscillatory response. However, the centralized inverted decoupling seems to have a better behaviour than the other two controllers.

3.2. An industrial-scale polymerization reactor

The second example is an industrial-scale polymerization reactor given by (36), where the time scales are in hours. The two controlled variables are measurements of the reactor condition and the two manipulated variables are the setpoints of the two reactors feed flow loops.

$$G_R(s) = \begin{pmatrix} \frac{22.89e^{-0.2s}}{4.572s+1} & \frac{-11.64e^{-0.4s}}{1.807s+1} \\ \frac{4.689e^{-0.2s}}{2.174s+1} & \frac{5.80e^{-0.4s}}{1.801s+1} \end{pmatrix} \quad (36)$$

In this case because of the time delays of the system, there is not any realizable configuration for centralized inverted decoupling, neither the scheme of Fig. 2 nor Fig. 3. To get realizability it is necessary to add an extra time delay associated to the first input. The diagonal block N(s) is given by $n_{11}(s)=e^{-0.2s}$ and $n_{22}(s)=1$. Then the new apparent process is the following

$$G_R^N(s) = \begin{pmatrix} \frac{22.89e^{-0.4s}}{4.572s+1} & \frac{-11.64e^{-0.4s}}{1.807s+1} \\ \frac{4.689e^{-0.4s}}{2.174s+1} & \frac{5.80e^{-0.4s}}{1.801s+1} \end{pmatrix} \quad (37)$$

As the process consists of FOPTD systems, the control design procedure is the same of the previous example, but using the new process (37). The time delay of both $l_i(s)$ is 0.4 hours and after specifying a gain margin of 5 in both loops, $k_i=0.785$ is obtained from (14). The resulting controller parameters are in table 3.

Table 3. Controller parameters for the polymerization reactor.

k(s)	K_P	K_I	K_D	N	τ
k_{11}	0.157	0.0343	0	0	0
k_{22}	0.244	0.1355	0	0	0
k_{12}	x	x	-14.82	1.807	0
k_{21}	x	x	5.97	2.174	0

Next, in order to verify the nominal control system performance, the closed loop system responses are shown in Fig. 6 (outputs) and Fig. 7 (control signals). There are unit steps changes in the references at t=1 h, in the first reference, and at t=25 h, in the second one. For comparison the PID decoupling control of Xiong [14] is also shown in these figures. The proposed design presents better performance. In the outputs the inverted control is better in terms of overshoot, decoupling and settling time. The control signals are less aggressive and their peaks are smaller.

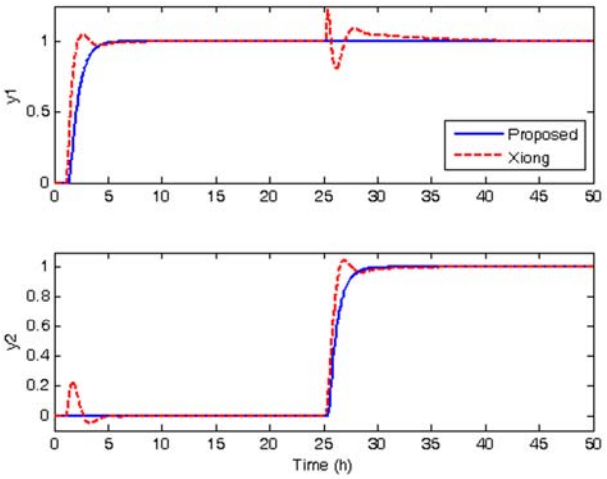

Figure 6: Outputs of the step response of polymerization reactor.

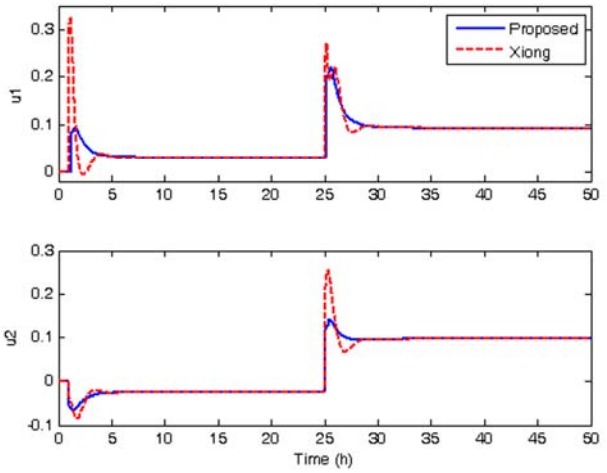

Figure 7: Control signals of the step response of polymerization reactor.

To investigate the robustness of the different controllers, all four time delays of the system are increased by 70% and the same previous test is carried out. The closed loop responses of outputs and control signals are shown in Fig. 8 and Fig. 9, respectively. Although there is a bit loss of decoupling, the performance of the proposed centralized inverted decoupling control is still better than the other control. The response is much less oscillatory.

3.3. The quadruple-tank process

The experimental process is a quadruple tank plant [18] of the lab of the department of Computer Science of the University of Córdoba. The outputs are the level of the lower tanks inside the range [0-35] cm, and the inputs are flow references of the secondary control loops that regulate the operation of the pumps, in the range [0-200] cm^3/s. The plant was configured in order to show interaction problems but without having multivariable RHP zeros, and then it was identified around the operation point y=[20 20] cm and u=[138 126] cm^3/s. The resultant model is given by (38). It has a RGA of 2.29.

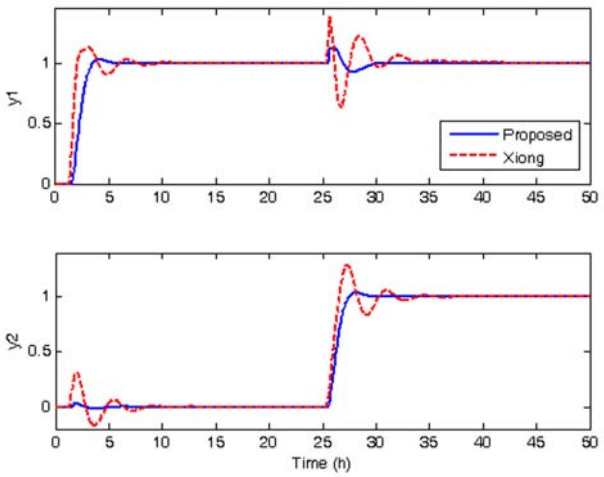

Figure 8: Outputs of the previous reactor with all time delays increased by 70%.

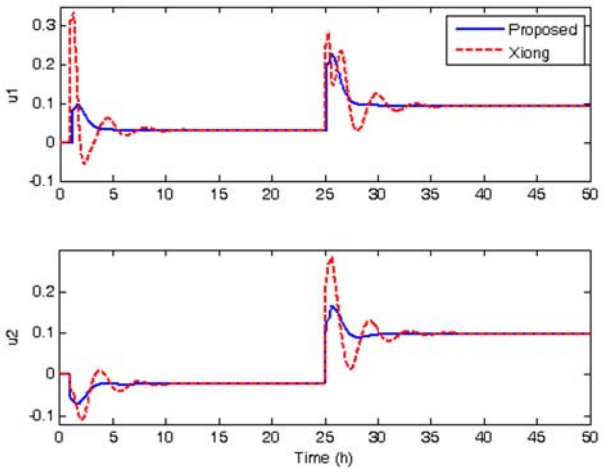

Figure 9: Control signals of the previous reactor with time delays increased by 70%.

$$G_T = \begin{pmatrix} \dfrac{0.3284}{184.5s+1} & \dfrac{0.2454}{(184.5s+1)(535.1s+1)} \\ \dfrac{0.2457}{(185s+1)(503.2s+1)} & \dfrac{0.3378}{185s+1} \end{pmatrix} \quad (38)$$

As the process is a stable and minimum phase system, the two open-loop transfer functions $l_1(s)$ y $l_2(s)$ are chosen following the first row of table 1. However, in this case the closed-loop transfer function is given by (15) because the time delays are all zero. Therefore, the specifications are in terms of the time constant $T_i = 1/k_i$ of the closed loop system. Time constants $T_1=T_2=300$ s are selected to obtain a settling time about 1500 s in both loops. So $k_1= k_2=1/300$. Using the expressions (24) and (25) the following controllers (39) are obtained. The diagonal elements are PI controllers. No approximation has been carried out in the other two.

$$k_{11}=1.873+\frac{1}{98.52s} \qquad k_{12}=\frac{-73.62s}{(184.5s+1)(535.1s+1)}$$
$$k_{21}=\frac{-73.71s}{(185s+1)(503.2s+1)} \qquad k_{22}=1.825+\frac{1}{101.34s} \quad (39)$$

The resultant step response of the closed-loop system is shown in Fig. 10 and Fig. 11 in comparison with the decentralized controller (40), which has been tuned for a phase margin of 90º and an infinite gain margin using the iterative methodology in [2]. The frequency bandwidth has been limited to $10^{-2.3}$.

$$k_{11}=3.44+\frac{1}{54.323s} \qquad k_{22}=3.35+\frac{1}{55.93s} \quad (40)$$

The proposed control achieves a better response with a very good decoupling performance in both loops. The decentralized control has a larger settling time and the rejection of the interactions is very slow.

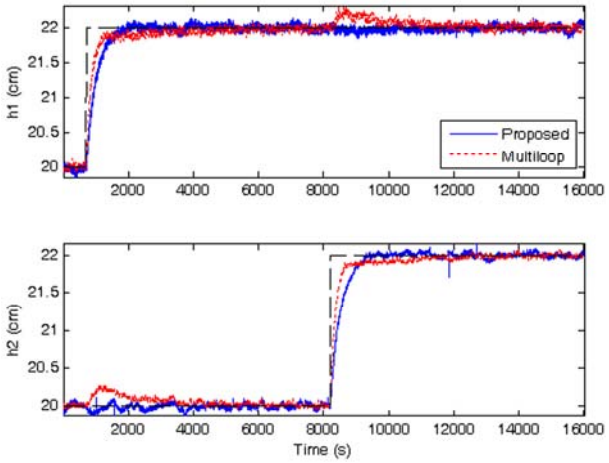

Figure 10: Outputs of the step response of the quadruple-tank process.

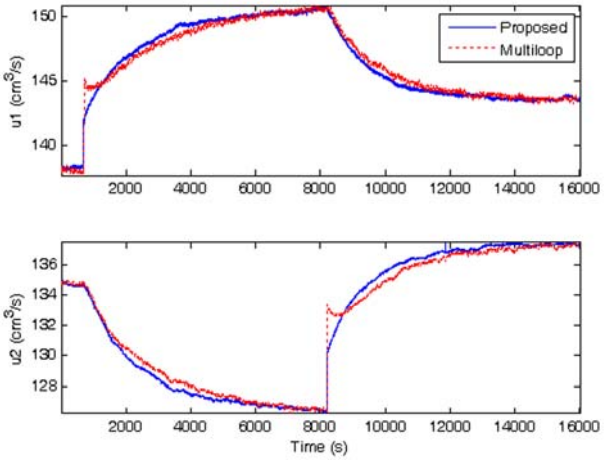

Figure 11: Control signal response of the quadruple-tank process.

4. Conclusions

A new approach of centralized control for TITO processes has been explained. The methodology is based on the controller structure of inverted decoupling. The main advantage is the simplicity of the four controller elements. In addition, it is possible to reduce them to two PID controllers and two filtered derivative compensators plus time delays, which can be easily implemented in commercial distributed control systems. The methodology has been illustrated with two representative

examples, found in multivariable literature, obtaining similar o better results than other authors. Also, it is applied to a real lab plant verifying its effectiveness.

Acknowledgements

This work has been supported by the Spanish CICYT under grant DPI 2007-62052. Moreover, J. Garrido thanks the FPU fellowship (Ref. AP2006-01049) of the Spanish Ministry of Education and Science.

References

[1] Aström, K. J.; Johansson, K. H.; Wang, Q. Design of decoupled PI controllers for two-by-two systems. IEE Proceedings control theory and applications, vol 149, pp. 74-81. 2002.

[2] Vázquez, F.; Morilla, F.; Dormido, S. An iterative method for tuning decentralized PID controllers. Proceeding of the 14th IFAC World Congress, pp. 491-496, 1999.

[3] Vázquez, F. Diseño de controladores PID para sistemas MIMO con control descentralizado. PhD Thesis. UNED, 2001.

[4] Vázquez, F.; Morilla, F. Tuning decentralized PID controllers for MIMO systems with decoupling. Proceeding of the 15th IFAC World Congress, pp. 2172-2178, 2002.

[5] Nordfeldt, P. PID Control of TITO Systems. Licentiate Thesis. Department of Automatic Control. Lund Institute of Technology, 2005

[6] Tavakoli S.; Griffin, I.; Fleming, P. J. Tuning of decentralised PI (PID) controllers for TITO processes. Control Engineering Practice 14, pp. 1069-1080, 2006.

[7] Wade, H. L. Inverted decoupling: a neglected technique. ISA Transactions 36, pp. 3-10, 1997.

[8] Waller, K. Decoupling in distillation. AIChE Journal Vol. 20, pp. 592-594, 1974.

[9] Lieslehto, J. MIMO controller design using SISO controller design methods. Proceeding of the 13th IFAC World Congress, pp. 169-173, 1996.

[10] Wang, Q. W.; Zhang, Y.; Chiu, M. S. Decoupling internal model control for multivariable systems with multiple time delays. Chemical Engineering Science Vol. 57, pp. 115-124, 2002.

[11] Wang, Q. W. Decoupling Control. Lecture Notes in Control and Information Sciences, 285, Springer-Verlag, 2003.

[12] Morilla, F.; Vázquez, F.; Garrido, J. Centralized PID Control by Decoupling for TITO Processes. Proceedings of 13th IEEE International Conference on Emerging Technologies and Factory Automation, pp. 1318-1325, 2008.

[13] Garrido, J.; Morilla, F.; Vázquez, F. Centralized PID Control by Decoupling of a Boiler-Turbine Unit. 10th European Control Conference, Budapest, 2009.

[14] Xiong, Q.; Cai, W. J.; He, M-J. Equivalent transfer function method for PI/PID controller design of MIMO processes. Journal of Process Control Vol. 17, pp. 665-673, 2009.

[15] Gagnon, E.; Pomerleau, A.; Desbiens, A. Simplified, ideal or inverted decoupling? ISA Transactions 37, pp. 265-276, 1998.

[16] Chen, P; Zhang, W. Improvement on an inverted decoupling technique for a class of stable linear multivariable processes. ISA Transactions 46, pp. 199-210, 2007.

[17] Wood, R. K.; Berry, M. W. Terminal composition control of a binary distillation column. Chemical Engineering Science, 28, pp. 1707-1717, 1973.

[18] Johansson, K. H.; Horch, A.; Wijk Olle; Hanssom A. Teaching multivariable control using the quadruple-tank process. IEEE Conference on Decision and Control, Phoenix, AZ, 1999..

Appendix A

Demonstration

$$\begin{aligned} y_1 &= g_{11}u_1 + g_{12}u_2 \\ y_2 &= g_{21}u_1 + g_{22}u_2 \end{aligned} \tag{A.1}$$

According to the control scheme of Fig. 2

$$\begin{aligned} u_1 &= k_{11}(r_1 - y_1) + k_{11}k_{12}u_2 = k_{11}e_1 + k_{11}k_{12}u_2 \\ u_2 &= k_{22}(r_2 - y_2) + k_{22}k_{21}u_1 = k_{22}e_2 + k_{22}k_{21}u_1 \end{aligned} \tag{A.2}$$

From (A.2)

$$\begin{aligned} u_1 &= \frac{k_{11}e_1 + k_{11}k_{12}k_{22}e_2}{1 - k_{11}k_{12}k_{21}k_{22}} \\ u_2 &= \frac{k_{22}e_2 + k_{22}k_{21}k_{11}e_1}{1 - k_{11}k_{12}k_{21}k_{22}} \end{aligned} \tag{A.3}$$

Substituting (A.3) into (A.1) leads to

$$\begin{aligned} y_1 &= \frac{k_{11}g_{11} + g_{12}k_{22}k_{21}k_{11}}{1 - k_{11}k_{12}k_{21}k_{22}}e_1 + \frac{k_{22}g_{12} + g_{11}k_{22}k_{12}k_{11}}{1 - k_{11}k_{12}k_{21}k_{22}}e_2 \\ y_2 &= \frac{k_{11}g_{21} + g_{22}k_{22}k_{21}k_{11}}{1 - k_{11}k_{12}k_{21}k_{22}}e_1 + \frac{k_{22}g_{22} + g_{21}k_{22}k_{12}k_{11}}{1 - k_{11}k_{12}k_{21}k_{22}}e_2 \end{aligned} \tag{A.4}$$

In order to get a diagonal L(s)=G(s)·K(s) in A.4, the expression of y_1 must be independent from e_2, and y_2 independent from e_1. Therefore,

$$\begin{aligned} k_{22}g_{12} + g_{11}k_{22}k_{12}k_{11} = 0 &\Rightarrow k_{11}k_{12} = \frac{-g_{12}}{g_{11}} \\ k_{11}g_{21} + g_{22}k_{22}k_{21}k_{11} = 0 &\Rightarrow k_{22}k_{21} = \frac{-g_{21}}{g_{22}} \end{aligned} \tag{A.5}$$

Then, substituting the expressions of (A.5) into (A.4)

$$\begin{aligned} y_1 &= k_{11}g_{11}e_1 = l_1e_1 \\ y_2 &= k_{22}g_{22}e_2 = l_2e_2 \end{aligned} \Rightarrow k_{11} = \frac{l_1}{g_{11}};\quad k_{22} = \frac{l_2}{g_{22}} \tag{A.6}$$

And finally, substituting (A.6) into (A.5)

$$k_{12} = \frac{-g_{12}}{l_1} \quad ; \quad k_{21} = \frac{-g_{21}}{l_2} \tag{A.7}$$